

## Understanding of phase modulation in two-level systems through inverse scattering

Andrew Hasenfeld, Sharon L. Hammes, and Warren S. Warren

Department of Chemistry, Princeton University, Princeton, New Jersey 08544-1009

(Received 25 November 1987)

Analytical and numerical calculations describe the effects of shaped radiation pulses on two-level systems in terms of quantum-mechanical scattering. Previous results obtained in the reduced case of amplitude modulation are extended to the general case of simultaneous amplitude and phase modulation. We show that an infinite family of phase- and amplitude-modulated pulses all generate rectangular inversion profiles. Experimental measurements also verify the theoretical analysis.

The understanding of the effects of an arbitrarily shaped radiation pulse on a two-level system is an old problem in quantum mechanics, but it still has tremendous practical importance in laser spectroscopy, nuclear magnetic resonance, and magnetic resonance imaging.<sup>1</sup> The case of constant field amplitude and no phase modulation was analytically solved half a century ago,<sup>2</sup> and provides the concept of pulse flip angle which is ubiquitous in coherent spectroscopy. This exact solution permits accurate calculation of the effects of any other pulse shape by breaking it up into enough rectangles. However, in practice one wishes to find pulse shapes which produce some *specific* desired excitation or inversion profile, and this inverse problem is quite complicated.

The only other complete analytic solution (all amplitudes, all resonance offsets) published to date is for the pulse envelope  $[\text{sech}(at)]^{1+\mu i}$ .<sup>3-5</sup> The qualitative behavior of the inversion profile from this unusual shape is vastly different from the rectangular pulse case. Above a certain minimum pulse amplitude the inversion profile is nearly rectangular, and remains theoretically (and experimentally<sup>6,7</sup>) unaffected as this amplitude is varied. The concept of a flip angle breaks down completely; no generalization for an arbitrarily phase- and amplitude-modulated shape has been found. Numerous other analytical results have been reported (for a review see Ref. 1) but all are restricted to one resonance offset or one amplitude, which drastically curtails their utility in realistic applications with inhomogeneities or multiple transitions. Approximate solutions have been found by numerical methods, but they provide little of the intuition which

will be necessary to ultimately generalize results to more complicated sequences.

In this paper we extend previous work on the inverse scattering reformulation of the Bloch equations<sup>8,9</sup> to include phase and amplitude modulated pulses. We show theoretically and experimentally that in this reformulation  $[\text{sech}(at)]^{1+5i}$  is only the first member of a multiply infinite family of phase- and amplitude-modulated pulses, all of which give the same inversion profile [in NMR parlance,  $I_z(\Delta\omega)$  starting from spin equilibrium]. That shape corresponds to a reflectionless potential<sup>10</sup> with a single bound state. The other waveforms involve more bound states, and have additional internal degrees of freedom. They take the spins along different trajectories, and can thus be more suitable for more sophisticated spectroscopic applications such as echo sequences. This formalism shows the surprising generality of raising an amplitude modulated envelope to a complex power, and provides additional insight into pulse shape design.

The basic physical motivation is to view Bloch evolution (in time  $t$ ) as a Schrödinger scattering process (in the spatial parameter  $\bar{x}$ , to avoid confusing the Schrödinger  $\bar{t}$  with the Bloch  $t$ ). While the exact theory<sup>11</sup> is on the infinite line  $[-\infty, \infty]$ , practical considerations demand a pulse shape compactly supported on an interval  $[0, T]$ . This is taken care of by ensuring that the pulse-shape tails are sufficiently small ( $\leq 10^{-4}$ ). The inverse scattering formalism for amplitude-modulated pulses has been derived elsewhere.<sup>8</sup> Here we start with the Bloch equations for amplitude and phase modulation

$$\frac{d}{dt} \begin{pmatrix} \langle \sigma_x \rangle \\ \langle \sigma_y \rangle \\ \langle \sigma_z \rangle \end{pmatrix} \equiv \begin{pmatrix} M_x \\ M_y \\ M_z \end{pmatrix} = \begin{pmatrix} 0 & \Delta\omega & -\omega_1(t) \sin\phi(t) \\ -\Delta\omega & 0 & \omega_1(t) \cos\phi(t) \\ \omega_1(t) \sin\phi(t) & -\omega_1(t) \cos\phi(t) & 0 \end{pmatrix} \begin{pmatrix} M_x \\ M_y \\ M_z \end{pmatrix}, \quad (1)$$

with the initial condition

$$\mathbf{M}(\Delta\omega, 0) = \begin{pmatrix} 0 \\ 0 \\ -1 \end{pmatrix},$$

and where relaxation terms are neglected. By stereographically projecting  $\mathbf{M}$  onto the  $y$ - $z$  plane,

$$\eta(\Delta\omega, t) = \frac{M_z + iM_y}{M_x - 1}, \quad (2)$$

we find that  $\eta$  satisfies a Riccati equation

$$\dot{\eta} = \left[ \frac{\omega_1 \sin\phi + i\Delta\omega}{2} \right] \eta^2 + (i\omega_1 \cos\phi) \eta + \left[ \frac{\omega_1 \sin\phi - i\Delta\omega}{2} \right]. \tag{3}$$

As previously shown,<sup>8</sup> one is then able to construct a function

$$g(\Delta\omega, t) \equiv \exp \left[ -\frac{1}{2} \int_{-\infty}^t \left( (\omega_1 \sin\phi + i\Delta\omega) \eta + i\omega_1 \cos\phi + \frac{\dot{\omega}_1 \sin\phi + \omega_1 \dot{\phi} \cos\phi}{\omega_1 \sin\phi + i\Delta\omega} \right) dt' \right], \tag{4}$$

that linearizes (3) into the form

$$\ddot{g} = \left[ -\left[ \frac{\omega_1}{2} \right]^2 - i \frac{\dot{\omega}_1 \cos\phi}{2} + i \frac{\omega_1 \dot{\phi} \sin\phi}{2} - \left[ \frac{\Delta\omega}{2} \right]^2 + O(\dot{\omega}_1^2) \right] g. \tag{5}$$

Finally, replacing the Bloch evolution parameter  $t$  by a spatial variable  $\bar{x}$  translates this into a Schrödinger scattering problem

$$-\frac{d^2 g}{d\bar{x}^2} + (V - E)g = 0, \tag{6}$$

where one identifies the energy  $E$  and potential  $V$  as

$$E \equiv \lambda^2 = \left[ \frac{\Delta\omega}{2} \right]^2, \quad V(\bar{x}) = -\left[ \frac{\omega_1}{2} \right]^2 - i \frac{\dot{\omega}_1 \cos\phi}{2} + i \frac{\omega_1 \dot{\phi} \sin\phi}{2} + O(\dot{\omega}_1^2) \tag{7}$$

and where  $O(\dot{\omega}_1^2)$  denotes “order of  $\dot{\omega}_1^2$ .” The inverse problem arises from the desire to find the field modulation  $\gamma H_1(t) = \omega_1(t) [\cos\phi(t)\hat{x} + \sin\phi(t)\hat{y}]$  that would realize a specific  $\mathbf{M}(\Delta\omega, T)$ . In contrast to the real-valued case of amplitude modulation<sup>8,9</sup> (in which only the single function  $\omega_1$  needs to be recovered), in this full case, we need to find both  $\omega_1$  and  $\phi$ , so that a complex potential is required.

The actual pulse occurs during a finite interval (extending from 0 to  $T$ ), and thus it vanishes as  $t \rightarrow \pm\infty$ . This translates into the spatial condition that  $V \rightarrow 0$  as  $\bar{x} \rightarrow \pm\infty$ . The initial condition

$$\mathbf{M}(\Delta\omega, 0) = \begin{pmatrix} 0 \\ 0 \\ -1 \end{pmatrix}$$

implies  $\eta = 1$ . So from Eq. (4),

$$g \sim \begin{cases} e^{-i\lambda\bar{x}} & \text{as } \bar{x} \rightarrow -\infty, \\ a(\lambda)e^{-i\lambda\bar{x}} + b(\lambda)e^{i\lambda\bar{x}} & \text{as } \bar{x} \rightarrow \infty. \end{cases} \tag{8}$$

In addition, we can impose boundary conditions on the bound states ( $E = -\lambda_i^2, \lambda_i > 0, i = 1, \dots, N$ )

$$g \sim \begin{cases} e^{\lambda_i\bar{x}} & \text{as } \bar{x} \rightarrow -\infty, \\ b_i(\lambda_i)e^{-\lambda_i\bar{x}} & \text{as } \bar{x} \rightarrow \infty, \end{cases} \tag{9}$$

where  $b_i$  is the  $i$ th normalization constant.

Equations (5)–(7) are perfectly general, but they do not lead to analytic solutions for arbitrary  $V$  and  $E$ , except in the special case of  $V$  a “reflectionless” potential.<sup>10</sup> It was shown explicitly in Ref. 9 that real reflectionless potentials with  $N$  bound states generate broadband  $2\pi N$  pulse shapes.  $N = 1$  is the McCall-Hahn  $\text{sech}(at)2\pi$  pulse;<sup>12</sup> the  $N = 2$  family generate broadband  $4\pi$  pulses, where the potential  $V$  has three adjustable parameters. All of these pulses generate no net excitation. The case of

a complex potential is normally much more involved. However, recall that we reconstruct  $\omega_1$  and  $\phi$  from the real and imaginary parts of  $V$ . Thus, from (7), if

$$\dot{\omega}_1 \sim \omega_1 \dot{\phi}, \tag{10}$$

we see that

$$\text{Re}(V) \sim -\left[ \frac{\omega_1}{2} \right]^2, \tag{11}$$

$$\text{Im}(V) \sim -\frac{\dot{\omega}_1}{2}(\cos\phi + \sin\phi),$$

so that the previously derived amplitude result<sup>8</sup> sits in  $\text{Re}(V)$  and the  $\text{Im}(V)$  contains the desired phase modulation. We therefore obtain from (10) the ansatz

$$\phi = \mu \ln(\omega_1), \tag{12}$$

for the phase modulation for constant  $\mu$ .

Moreover, by examining the large  $t$  behavior of  $\dot{g}/g$ , one can show that  $V$  in (11) is a reflectionless potential, and that the only allowed final states are  $M_z = \pm 1$ .<sup>11</sup> From (11), we have that  $\omega_1 \sim \sqrt{-\text{Re}(V)}$ , and combining with (12), we obtain the ansatz

$$\gamma H_1(t) = \omega_1 e^{i\mu \ln(\omega_1)} = \omega_1^{(1+\mu i)} \sim (\sqrt{-V})^{(1+\mu i)}, \tag{13}$$

for  $V$  a reflectionless potential. Potentials of the form of Eq. (13) yield simple scattering behavior. In fact, over a wide range of pulse parameters their inversion performance is nearly *identical*.

We show numerical simulations<sup>13</sup> of the Bloch equations (1) using this ansatz. The analytic approach above is exact in the limit as  $t \rightarrow \pm\infty$ , but in our finite numerical simulations the behavior is not perfect (i.e., there is a transition region from  $M_z = -1$  to  $M_z = 1$ ). Nevertheless, as shown in Figs. 1–3, the behavior is very close to the limiting theoretical results. In Fig. 1 we see the pulse

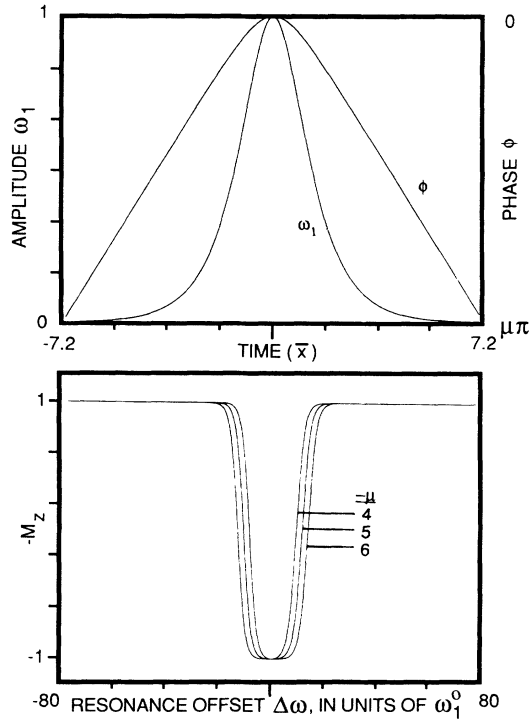


FIG. 1. The  $N=1$  reflectionless potential at the top is used in the ansatz (13) as an inverting pulse, where the response  $-M_z$  is displayed as a function of resonance offset  $\Delta\omega/\omega_1^0$  at the bottom. Note that in Figs. 1-3, the eigenvalues are given by  $\lambda_i = N - i + 1$ , and  $\omega_1^0$  denotes the average pulse height.

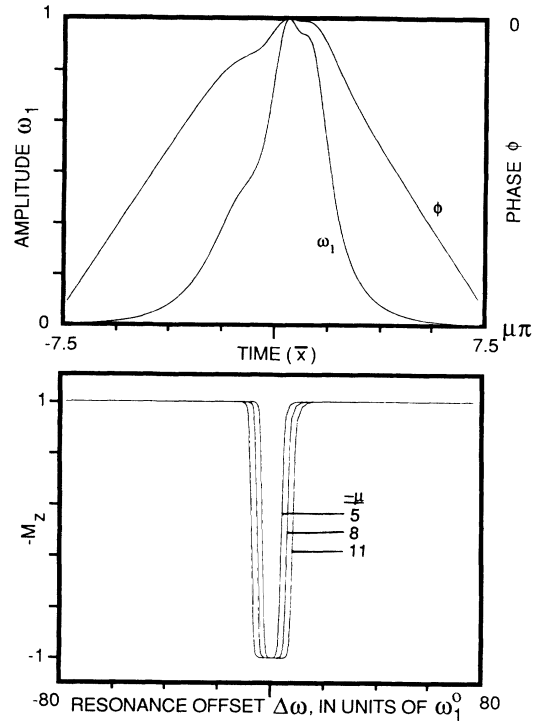


FIG. 3. The  $N=3$  reflectionless potential at the top is used in the ansatz (13) as an inverting pulse, where the response  $-M_z$  is displayed as a function of resonance offset  $\Delta\omega/\omega_1^0$  at the bottom.

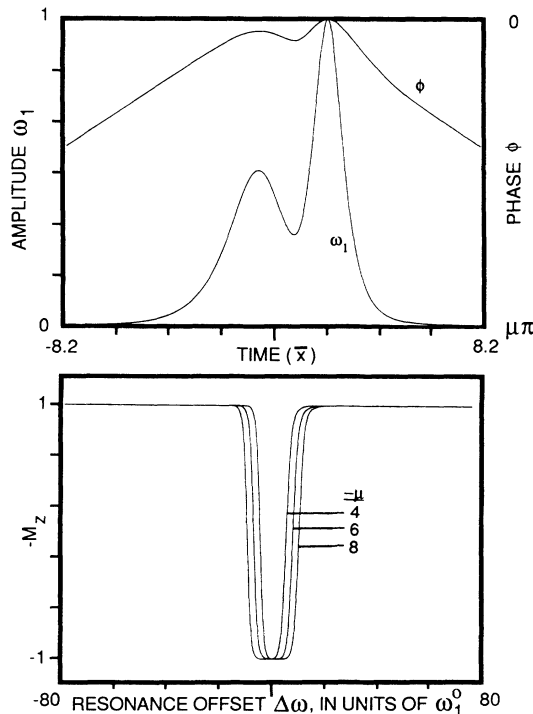


FIG. 2. The  $N=2$  reflectionless potential at the top is used in the ansatz (13) as an inverting pulse, where the response  $-M_z$  is displayed as a function of resonance offset  $\Delta\omega/\omega_1^0$  at the bottom.

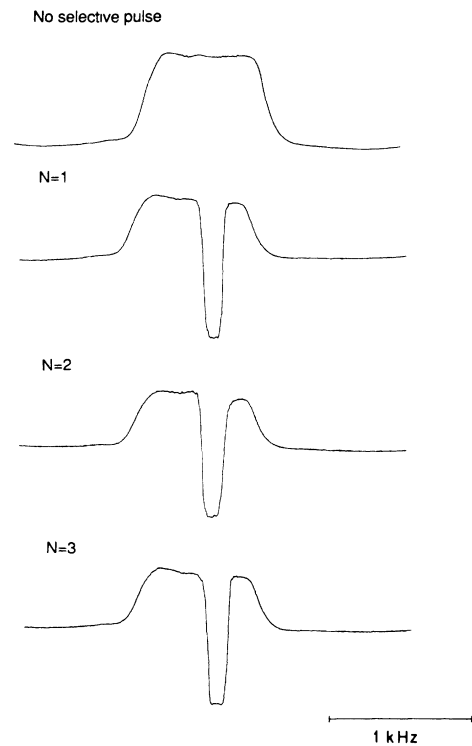


FIG. 4. Experimental verification, utilizing an inhomogeneously broadened line from a water sample in a 270 MHz spectrometer, is shown for the three pulses given in Figs. 1-3 (for  $-\mu=5$ ).

generated from the only reflectionless potential with  $N=1$  (one bound state), which becomes  $[\text{sech}(at)]^{1+\mu i}$ . Figures 2 and 3 show examples of  $N=2$  and  $N=3$  potentials. In the general case, the pulse arising from an  $N$  bound-state potential has  $2N-1$  adjustable parameters (the  $N$  eigenvalues and  $N$  normalization constants, modulo translations), which along with the phase modulation parameter  $\mu$  can vary continuously over a broad range.<sup>11</sup> Figure 4 shows the experimental inversion profiles from the shapes in Figs. 1-3.

One can understand the response purely in terms of scattering, with no need to appeal to the concept of adiabatic rapid passage.<sup>14</sup> Loosely speaking, a wave incident on a potential behavior of height  $\sim \omega_f^2$  with energy  $\sim \Delta\omega^2$  will be exponentially damped if the energy in the wave is too small (corresponding to  $M_z = 1$ ). Likewise, when the energy of the wave surpasses the height of the barrier,

there is no reflection, and the wave propagates unimpeded (corresponding to  $M_z = -1$ ). The transition occurs when the energy in the wave is close to the height of the barrier. It is clear that there is a compelling correspondence between the behavior of two-level systems and elementary quantum-mechanical scattering.

One of us (A.H.) gratefully acknowledges enlightening conversations with M. Kruskal, and thanks the Princeton Local Allocation Committee for five hours of superconductor time at the John von Neumann Center. We also thank M. McCoy for his experimental expertise. This work was supported by the National Institutes of Health under Grant No. GM35253 BBCB, by the National Science Foundation under Grant No. CHE-8502199, and (for W.S. Warren) by the Alfred P. Sloan Foundation.

<sup>1</sup>W. S. Warren and M. S. Silver, *Adv. Magn. Reson.* **12**, 247 (1988).

<sup>2</sup>I. I. Rabi, *Phys. Rev.* **51**, 652 (1937).

<sup>3</sup>L. Allen and J. H. Eberly, *Optical Resonance and Two-level Atoms* (Wiley, New York, 1975).

<sup>4</sup>M. S. Silver, R. I. Joseph, and D. I. Hoult, *Phys. Rev. A* **31**, 2753 (1985).

<sup>5</sup>F. T. Hioe, *Phys. Rev. A* **30**, 2100 (1984).

<sup>6</sup>C. P. Lin, J. Bates, J. Mayer, and W. S. Warren, *J. Chem. Phys.* **86**, 3750 (1987).

<sup>7</sup>M. S. Silver, R. I. Joseph, and D. I. Hoult, *J. Magn. Reson.* **59**, 347 (1984).

<sup>8</sup>F. A. Grünbaum and A. Hasenfeld, *Inverse Probl.* **2**, 75 (1986).

<sup>9</sup>A. Hasenfeld, *J. Magn. Reson.* **72**, 509 (1987).

<sup>10</sup>V. Bargmann, *Rev. Mod. Phys.* **21**, 488 (1949).

<sup>11</sup>A. Hasenfeld, in *Signal Processing*, The IMA volumes on Mathematics and its Applications, edited by L. Auslander, S. Mittel, and P. Khargoneker (Springer, New York, in press).

<sup>12</sup>S. L. McCall and E. L. Hahn, *Phys. Rev.* **183**, 457 (1969).

<sup>13</sup>A. Hasenfeld, *Magn. Reson. Med.* **2**, 505 (1985).

<sup>14</sup>A. Abragam, *The Principles of Nuclear Magnetism* (Oxford Univ. Press, London, 1961), p. 65.